Molecular Pharmacology Fast Forward. Published on July 28, 2020 as DOI: 10.1124/mol.120.119453
This article has not been copyedited and formatted. The final version may differ from this version.

A truncated six transmembrane splice variant MOR-1G enhances expression of the full-length seven transmembrane mu opioid receptor through heterodimerization

Tiffany Zhang, Jin Xu, and Ying-Xian Pan

Department of Neurology and the Molecular Pharmacology and Chemistry Program

(TZ, JX, YXP)

Memorial Sloan-Kettering Cancer Center, New York, NY 10065, USA

Molecular Pharmacology Fast Forward. Published on July 28, 2020 as DOI: 10.1124/mol.120.119453
This article has not been copyedited and formatted. The final version may differ from this version.

Running title: Truncated 6TM variant enhances 7TM mu opioid receptor expression

Corresponding author:

Ying-Xian Pan, MD PhD

Member

Department of Neurology

Memorial Sloan Kettering Cancer Center

1275 York Ave

New York, NY 10065

pany@mskcc.org

Pages: 42

Figures: 4

Tables: 2

Words

Abstract: 228

Introduction: 481

Discussion: 1503

References: 43

Abbreviations:

OPRM1, mu opioid receptor gene; mMOR-1, mouse mu opioid receptor; mMOR-1G, mouse mu opioid receptor-1G; mMOR-1/Flag, Flag-tagged mMOR-1; mMOR-1G/HA, HA-tagged mMOR-1G; TM, transmembrane; KO, knockout; DAMGO, [D-Ala^2,MePhe^4,Gly(ol)^5]enkephalin; IBNtxA, 3-iodobenzoyl-6β-naltrexamide; BFA, brefeldin A; ER, endoplasmic reticulum; GPCR, G protein-coupled receptor; GTPγS, guanosine 5'-3-*O*-(thio)triphosphate; qPCR, quantitative PCR; ANOVA, analysis of variance.

Molecular Pharmacology Fast Forward. Published on July 28, 2020 as DOI: 10.1124/mol.120.119453
This article has not been copyedited and formatted. The final version may differ from this version.

Abstract

The mu opioid receptor gene, *OPRM1*, undergoes extensive alternative splicing to generate an array of splice variants. One group of splice variants exclude the first transmembrane (TM) domain and contain six TM domains. These 6TM variants are essential for the action of a novel class of analgesic drugs, including 3-iodobenzoyl-6β-naltrexamide (IBNtxA), which is potent against a spectrum of pain models without exhibiting the adverse side effects of traditional opiates. The 6TM variants are also involved in analgesic action through other drug classes, including delta and kappa opioids, and α_2-adrenergic drugs. Of the five 6TM variants in mouse, mMOR-1G is abundant and conserved from rodent to human. In the present study, we demonstrate a new function of mMOR-1G in enhancing expression of the full-length 7TM mu opioid receptor, mMOR-1. When co-expressed with mMOR-1 in a Tet-Off inducible Chinese Hamster Ovary cell line, mMOR-1G has no effect on mMOR-1 mRNA expression, but greatly increases mMOR-1 protein expression in a dose-dependent manner, determined by opioid receptor binding and [^{35}S]GTPγS binding. Subcellular fractionation analysis using OptiPrep density gradient centrifugation shows an increase of functional mMOR-1 receptor in plasma membrane-enriched fractions. Using a co-immunoprecipitation approach, we further demonstrate that mMOR-1G physically associates with mMOR-1 starting at the endoplasmic reticulum, suggesting a chaperone-like function. These data provide a molecular mechanism for how mMOR-1G regulates expression and function of the full-length 7TM mu opioid receptor.

Molecular Pharmacology Fast Forward. Published on July 28, 2020 as DOI: 10.1124/mol.120.119453
This article has not been copyedited and formatted. The final version may differ from this version.

Significance Statement

The current study establishes a novel function of mMOR-1G, a truncated splice variant with six transmembrane domains (TM) of the mouse mu opioid receptor gene, in enhancing expression of the full-length 7TM mMOR-1 through a chaperone-like function.

Molecular Pharmacology Fast Forward. Published on July 28, 2020 as DOI: 10.1124/mol.120.119453
This article has not been copyedited and formatted. The final version may differ from this version.

Introduction

The mu opioid receptor has a special place in the opioid receptor family since it mediates most clinically relevant opioids such as morphine and fentanyl, as well as heroin. The single-copy mu opioid receptor gene (*OPRM1*) undergoes extensive alternative pre-mRNA splicing, producing multiple splice variants or isoforms with a pattern that is conserved from rodent to human (Pan, 2005; Pasternak and Pan, 2013). These splice variants can be categorized into three structurally distinct types: 1) full-length 7 transmembrane (TM) Carboxyl (C) terminal variants; 2) truncated 6TM variants excluding the first TM; and 3) truncated single TM variants that contain only the first TM (Pasternak and Pan, 2013).

The functional significance of the full-length 7TM C-terminal variants has been demonstrated by differences in regional- and/or cell-specific expression, mu agonist-induced G protein coupling, phosphorylation, internalization and post-endocytic sorting, as well as *in vivo* morphine activity (Abbadie et al., 2000a; Abbadie et al., 2000b; Abbadie et al., 2004; Bolan et al., 2000; Caron et al., 2000; Koch et al., 2001; Koch et al., 1998; Pan et al., 2001a; Pan et al., 1999; Tanowitz et al., 2008; Xu et al., 2017). The truncated single TM variants do not bind any opioids. Rather, they function as molecular chaperones that facilitate expression of the 7TM MOR-1 receptor and enhance morphine analgesia (Xu et al., 2013).

Using *Oprm1* gene targeting mouse models, we previously demonstrated the functional importance of the truncated 6TM variants in mediating a novel class of opioids, such as 3-iodobenzoyl-6β-naltrexamide (IBNtxA) (Majumdar et al., 2011b; Majumdar et al., 2012) IBNtxA is potent against thermal, inflammatory and neuropathic

Molecular Pharmacology Fast Forward. Published on July 28, 2020 as DOI: 10.1124/mol.120.119453
This article has not been copyedited and formatted. The final version may differ from this version.

pain in animal models, and does not produce respiratory depression, physical dependence or reward behavior (Majumdar et al., 2011b; Wieskopf et al., 2014). In an *Oprm1* exon 11-knockout (KO) mouse model devoid of all 6TM variants with preservation of 7TM C-terminal variants, IBNtxA analgesia was completely eliminated while morphine analgesia was preserved (Majumdar et al., 2011a; Majumdar et al., 2011b). Conversely, in a triple KO mouse model lacking mu exon 1-associated 7TM variants, delta receptors and kappa receptors (Schuller et al., 1999), morphine analgesia was completely abolished, but IBNtxA analgesia remained intact (Majumdar et al., 2011a; Majumdar et al., 2011b; Pasternak and Pan, 2013). Gain of function studies further confirmed that 6TM variants are both necessary and sufficient for IBNtxA analgesia (Lu et al., 2015; Lu et al., 2018). In a complete mu opioid receptor (*Oprm1*) KO mouse lacking both 7TM and 6TM variants, both morphine and IBNtxA analgesia were lost. Restoring expression of any of the individual 6TM variants through lentiviral-mediated delivery in the complete *Oprm1* KO mice rescued IBNtxA, but not morphine, analgesia.

The current study establishes a novel function of mMOR-1G, a conserved and dominant 6TM variant, in enhancing expression of the full-length 7TM mMOR-1 at the protein level through heterodimerization, providing new insights into the roles of the 6TM variants in mu opioid pharmacology.

Molecular Pharmacology Fast Forward. Published on July 28, 2020 as DOI: 10.1124/mol.120.119453
This article has not been copyedited and formatted. The final version may differ from this version.

Materials and Methods

Materials. [^{3}H][D-Ala^{2},*N*-MePhe^{4},Gly(ol)^{5}] enkephalin (DAMGO, 53.4 Ci/mmol), [^{35}S] GTPγS (1250 Ci/mmol) was purchased from PerkinElmer (Boston, MA). Opiates and opioid peptides were a generous gift from the Research Technology Branch of the National Institute on Drug Abuse Drug Supply Program (Rockville, MD). Be(2)C cells were obtained from ATCC, while Tet-off Chinese Hamster Ovary (CHO) cells were obtained from Clontech (Mountain View, CA). The oligodeoxynucleotides were synthesized and purified through Sigma-Aldrich (St. Louis, MO). The anti-Flag antibody, EZview Red Anti-Flag M2, EZview Red Anti-HA Affinity Gels, 3x Flag peptide and HA peptide were from Sigma-Aldrich. The anti-HA antibody and Anti-glyceraldehyde 3-phosphate dehydrogenase (GAPDH) antibody were from Cell Signaling (Beverly, MA). All other materials were obtained from the sources listed.

Reverse transcription and quantitative polymerase chain reaction (RT-qPCR). Total RNA was isolated from Tet-off CHO cells with the RNeasy Kit (Qiagen) and treated with DNAse I using Turbo DNA-free Reagents (Invitrogen). Reverse transcription with random primers and Superscript II reverse transcriptase (Invitrogen) were performed as described previously (Xu et al., 2013). SYBR qPCR with the Hot start SYBR Green Master Mix (Affimetrix, Santa Clara, CA) was then carried out in the CFX96 machine (Bio-Rad), using the first-strand cDNAs as the template. qPCR primers were as follows: sense primer-1 (SP-1), 5'-GCC CTC TAT TCT ATC GTG TGT GTA GTG G-3' and antisense primer-1 (AP-1), 5'-CAA TCT ATG GAC CCC TGC CTG TAT TTT G-3', for mMOR-1; SP-2, 5'-GAT CTG GGC CGA TGA TGG AAG CTT TC-3' and AP-1, for mMOR-1G. qPCRs of the glyceraldehyde 3-phosphate dehydrogenase

Molecular Pharmacology Fast Forward. Published on July 28, 2020 as DOI: 10.1124/mol.120.119453
This article has not been copyedited and formatted. The final version may differ from this version.

(G3PDH) (SP-3, 5'-ACC ACA GTC CAT GCC ATC AC-3' and AP-2, 5'-TCC ACC ACC CTG TTG CTG TA-3') and mouse 18S ribosome (m18S) (SP-4, 5'-GTA ACC CGT TGA ACC CCA TT-3' and AP-3, 5'-CCA TCC AAT CGG TAG TAG CG-3') were used as reference genes to calculate the normalization factor (NF) ($NF = (C(t)_{G3PDH} \times C(t)_{m18S})^{1/2}$ (Xu et al., 2014). The PCR program was 2 minutes at 95°C, followed by 45 cycles of a 15-second denaturing step at 95°C, a 30-second annealing step at 65°C (60°C for G3PDH and m18S), and a 30-second (1-minute for G3PDH and m18S) extension at 72°C, followed by melting curve analysis. mMOR-1 and mMOR-1G expression levels were calculated with the equation $2^{-\Delta(Ct)}$ ($\Delta C(t) = C(t)_{mMOR\text{-}1 \text{ or } mMOR\text{-}1G} - NF$) and normalized to samples treated with 100 ng/ml of doxycycline.

Cell culture, plasmid constructs, and stable or transient transfection. The *OPRM1*-knockdown (KD) Be(2)C cell line was cultured in MEM with non-essential amino acids:F12, 10% FCS and 0.1 mg/ml hygromycin. This *OPRM1*-KD cell line was made by stably expressing two shRNA constructs in the pSilencer 2.1-U6 hygro vector (Ambion) that specifically targeted human MOR-1 exons 1, but not mouse exon 1, in Be(2)C cells (ATCC), a human neuroblastoma line that contains endogenous *OPRM1* splice variants, with hygromycin selection. The constructs were made by annealing and subcloning two pairs of oligos (A: sense oligo, 5'-GAT CCG CGC CAG CAA TTG CAC TGA TTT CAA GAG AAT CAG TGC AAT TGC TGG CGT TTT TTG GAA A-3' and antisense oligo, 5'-AGC TTT TCC AAA AAA CGC CAG CAA TTG CAC TGA TTC TCT TGA AAT CAG TGC AAT TGC TGG CGC G-3'; B: sense oligo, 5'-GAT CCG CTT GTC CCA CTT AGA TGG CTT CAA GAG AGC CAT CTA AGT GGG ACA AGT TTT TTG GAA A-3' and antisense oligo, 5'-AGC TTT TCC AAA AAA CTT GTC CCA CTT AGA

Molecular Pharmacology Fast Forward. Published on July 28, 2020 as DOI: 10.1124/mol.120.119453
This article has not been copyedited and formatted. The final version may differ from this version.

TGG CTC TCT TGA AGC CAT CTA AGT GGG ACA AGC G-3') into pSilencer 2.1-U6 hygro with the restriction enzymes BamHI and HindIII. The selected stable cells were then screened with [^{3}H] DAMGO binding, and a cell line with a 99% reduction in binding was used for transient transfection experiments. C-terminal HA tagged mMOR-1G constructs were made by first performing PCR with primers containing the HA tag sequence and then subcloning the PCR fragments into the pcDNA3.1 vector. C-terminal Flag tagged mMOR-1 constructs were made by subcloning mMOR-1 cDNA into p3XFLAG-CMV-14 vectors (Sigma-Aldrich).

Transient transfections in *OPRM1*-KD Be(2)C cells were carried out in 100 mm plates with Fugene HD (Promega) following the manufacturer's protocol. Equal amounts of Flag-tagged mMOR-1 (mMOR-1/Flag) and HA-tagged mMOR-1G (mMOR-1G/HA) constructs were used in co-transfection. In transfections with a single construct, the amount of mMOR-1/Flag or mMOR-1G/HA construct used was the same as in co-transfection, and pcDNA3.1 vector DNA without any insertion was included so the total amount of DNA in each transfection was preserved. The cells were harvested 32 -36 hours after transfection and used for solubilization and immunoprecipitation or membrane preparation.

Tet-off CHO cells were cultured in MEMα with 2 mM glutamine media, 10% Tet-free fetal calf serum (FCS) (Clontech), and 0.1 mcg/ml G418. mMOR-1 and mMOR-1G cDNAs were subcloned into the pcDNA3.1 (Invitrogen) and pTRE2hyg vector (Clontech) with appropriate restriction enzymes, respectively. To generate the Tet-off CHO stable cell line, Tet-off CHO cells were co-transfected with mMOR-1 and mMOR-1G constructs using the LipofectAMINE reagent (Invitrogen) and selected with G418 (0.9 mcg/ml) and

Molecular Pharmacology Fast Forward. Published on July 28, 2020 as DOI: 10.1124/mol.120.119453
This article has not been copyedited and formatted. The final version may differ from this version.

hygromycin (0.6 mg/ml) for two weeks. The stable cells were then treated with doxycycline for 48-72 hours to suppress mMOR-1G expression before they were harvested for opioid receptor binding, [^{35}S]GTPγS binding and RT-qPCR. All cells were grown at 37°C in a 5% CO_2/95% air humidified atmosphere.

Opioid receptor binding assays. Tet-off cells grown under indicated doxycycline concentrations were harvested for membranes as previously described (Pan et al., 1999), and protein concentration was determined with the Lowry method. [^{3}H]DAMGO binding was carried out at 25°C for 60 min in 7.4 pH buffer containing 50 mM potassium phosphate and 5 mM magnesium sulfate. The incubation was then rapidly filtered with glass fiber filter paper and washed three times with 3 mL of ice-cold filtering buffer (50 mM Tris-HCl, pH 7.4). Bound radioactivity was extracted in 3 mL of Liquiscint scintillation fluid overnight before being determined by liquid scintillation spectrophotometry. Specific binding was defined as the difference between total binding and nonspecific binding, defined by 10 uM levallorphan. Nonlinear regression analyses (GraphPAD Prism 7, San Diego, CA) was used to calculate K_D and K_i values.

[^{35}S]GTPγS binding. 30 µg of membrane protein from cells were incubated in the presence and absence of various concentrations (0.01 – 30 µM) of different mu opioids and opioid peptides for 60 min at 30°C in the assay buffer (50 mM Tris/HCL, pH 7.7, 3 mM $MgCl_2$, 0.2 mM EGTA, 10 mM NaCl) containing ~ 0.05 mM [^{35}S]GTPγS and 60 µM GDP, as described previously (Pan et al., 2005). The incubation was then filtered through glass fiber filter paper and washed three times with ice cold filtering buffer. Basal binding was assessed in the presence of GDP and absence of drug. EC_{50} and %

Molecular Pharmacology Fast Forward. Published on July 28, 2020 as DOI: 10.1124/mol.120.119453
This article has not been copyedited and formatted. The final version may differ from this version.

stimulation values over basal level were calculated by nonlinear regression analysis (GraphPad Prism 7).

Immunoprecipitation and Western blot analyses. Whole cells from the transient transfection were solubilized in lysis buffer A (phosphate-buffered saline (PBS), pH7.4, 8 mM CHAPS and a protease inhibitor cocktail of 2 µg/ml each leupeptin, pepstatin, aprotinin, and bestatin, and 0.2 mM phenylmethylsulfonyl fluoride (PMSF)), with shaking at 4°C for 5 h. The mixture was then centrifuged for 15 minutes at 13,000g and 4°C before the supernatant was incubated with either EZview Red Anti-Flag (M2) or EZview Red Anti-HA beads and shaken overnight at 4°C. The affinity gels were then washed with wash buffer (PBS, pH 7.4, 5 mM CHAPS), and then eluted with 3x FLAG peptide or HA peptide. The eluted sample was mixed with SDS sample buffer containing 0.15 M Dithiothreitol (DTT) and heated at 100°C for 10 min. The samples were then run on an Any kD SDS-PAGE gel (Bio-Rad) before blot transfer onto PVDF membranes. The membranes were shaken in a blocking buffer containing TTBS (10mM Tris–HCl, pH 7.4, 150mM NaCl, and 0.05% Tween 20), 4% nonfat dried milk, and 1% BSA at 25°C for 1 h and then incubated overnight with either the anti-HA antibody (1:1000), the anti-FLAG antibody (1:800 dilution), or the anti-GAPDH antibody (1:3000 dilution) in the blocking buffer at 4°C. After four washes with TTBS buffer for five minutes each, the membrane was incubated for 1 h at 25°C in TTBS with either peroxidase-conjugated goat anti-rabbit or goat-anti-mouse IgG antibody (1:10,000 dilution, Jackson ImmunoResearch). After washing another four times with TTBS buffer, the signals were visualized with ChemiGrow reagents (Proteinsimple, Santa Clara, CA), and imaged and analyzed on ChemiDoc MP Image System (Bio-Rad).

Molecular Pharmacology Fast Forward. Published on July 28, 2020 as DOI: 10.1124/mol.120.119453
This article has not been copyedited and formatted. The final version may differ from this version.

Brefeldin A (BFA) treatment. *OPRM1*-KD Be(2)C cells were transiently co-transfected with mMOR-1/Flag and mMOR-1G/HA. Eight hours after transfection, the cells were treated with or without 4 µg/ml of BFA for another 24 hours. The whole cells were then harvested and used for either immunoprecipitation and Western blot analysis or for membrane preparation used in [^{3}H]DAMGO binding, as described above.

Subcellular fractionation analysis. The Tet-Off cells stably expressing mMOR-1 and mMOR-1G treated with 100 ng/ml of doxycycline for 36 hrs or without doxycycline were lifted from 150 mm plates by incubating with 2 mM EDTA for 5 min at 37°C. After washing with PBS, the cell pellets were homogenized with a tight-fitting Dounce homogenizer for 25 strokes in Buffer A (10 mM Tris/HCl, pH7.4, 1 mM EDTA, 0.25 M sucrose and the protease inhibitor cocktail (see above)) and then passed through a 25-gauge syringe needle. Post-nuclear supernatant was collected by centrifugation of the pass through at 1,000 x g for 5 min and loaded on the top of the discontinuous OptiPrep (Fisher Scientific) gradient that was manually made by layering 1.4 ml each of 26%, 22%, 18%, 14%, 10%, 6% and 2% OptiPrep in Buffer A from the bottom of ultracentrifuge tube. After centrifugation at 284,000 x g for 3 hrs in a SORVALL wX+ Ultra Series centrifuge, sequential 0.8 ml fractions were harvested from the top of the tube and used for Western blot analysis and [^{3}H]DAMGO binding. The OptiPrep density in each fraction was determined by using absorbance 340 nm measurement following the manufacturer's instructions (Axis-Shield).

Statistical analysis. All statistical analysis was carried out using GraphPad Prism 7. Two-tailed Student *t*-test and one-way or two-way ANOVA with *post hoc* Bonferroni's multiple comparisons test were performed as described in the figure legend. Data

Molecular Pharmacology Fast Forward. Published on July 28, 2020 as DOI: 10.1124/mol.120.119453
This article has not been copyedited and formatted. The final version may differ from this version.

represented the means ± SD of at least three independent experiments. Statistical significance was set at $p < 0.05$.

Molecular Pharmacology Fast Forward. Published on July 28, 2020 as DOI: 10.1124/mol.120.119453
This article has not been copyedited and formatted. The final version may differ from this version.

Results

6TM variant mMOR-1G enhances expression of the functional 7TM mMOR-1 receptor protein in a Tet-Off CHO cell line

To investigate the influence of 6TM variants on the expression of 7TM mMOR-1, we generated a stable Tet-Off CHO cell line in which 7TM mMOR-1 is constitutively expressed, while the expression of the 6TM variant, mMOR-1G, is regulated by doxycycline, a synthetic drug derived from tetracycline. In contrast to a Tet-On system, the Tet-Off system uses doxycycline (Doxy) to suppress expression of a gene of interest (GOI), which was mMOR-1G in our study. Thus, in the absence of doxycycline, mMOR-1G is maximally expressed, while increased doxycycline concentration results in reduced expression of mMOR-1G. There are multiple 6TM variants of the mouse *Oprm1* gene. We selected mMOR-1G for this study because it was abundant and uniquely conserved from rodent to human. 6TM variants alone do not bind to available radio-labeled opioids, including [^{3}H]DAMGO, [^{3}H]diprenorphine and [^{125}I]IBNtxA when expressed in CHO cells (Fig. S1) or HEK293 cells (data not shown). Therefore, we used an opioid receptor binding assay with [^{3}H]DAMGO to determine the expression level of 7TM mMOR-1 protein, as [^{3}H]DAMGO binding represents the expression of only 7TM mMOR-1 protein, and not 6TM variants in this Tet-Off cell line co-expressing mMOR-1 and mMOR-1G. We also generated another Tet-Off cell line expressing only mMOR-1G regulated by doxycycline and lacking expression of 7TM mMOR1. In this mMOR-1G only Tet-Off cell line, there is no [^{3}H]DAMGO or [^{125}I]IBNtxA binding, with or without doxycycline (Fig. S2).

Molecular Pharmacology Fast Forward. Published on July 28, 2020 as DOI: 10.1124/mol.120.119453
This article has not been copyedited and formatted. The final version may differ from this version.

In the Tet-Off cell line with constitutive expression of 7TM mMOR-1 and doxycycline-regulated expression of mMOR-1G, we first observed that expression of mMOR-1G increased [^{3}H]DAMGO binding in a dose-dependent manner (Fig. 1A). When expression of mMOR-1G mRNA was fully suppressed by 100 ng/ml of doxycycline (Fig. 1C), a minimal level of [^{3}H]DAMGO binding was observed, which represents the basal or constitutive expression level of 7TM mMOR-1. However, when mMOR-1G mRNA was increased by lowering doxycycline (Fig. 1C), [^{3}H]DAMGO binding increased in parallel, reaching a maximum when no doxycycline was present and mMOR-1G mRNA was fully expressed. Saturation studies with [^{3}H]DAMGO further demonstrated an increase in functional receptor number (B_{max}), while receptor affinity (K_D) was unaffected (Table 1). However, mMOR-1 mRNA level was not significantly altered by different doses of doxycycline or mMOR-1G expression (Fig. 1B), suggesting that increased [^{3}H]DAMGO binding does not result from changes in mMOR-1 mRNA levels.

We then performed [^{35}S]GTPγS binding assays to assess the effect of 6TM mMOR-1G on modulating mu agonist-induced G protein coupling with mMOR-1 in the Tet-off CHO cell line co-expressing mMOR-1 and mMOR-1G. When compared to no mMOR-1G expression (+ Doxy), induction of mMOR-1G at maximal level (- Doxy) showed no significant effect on drug potency (EC_{50} value) of morphine, morphine-6β-glucuronide (M6G) and β-endorphin, but led to a small and significant decrease of the EC_{50} value for DAMGO. Meanwhile, the percent stimulation over basal level (% Stim), an indication of drug efficacy, by morphine, DAMGO and M6G, increased significantly when mMOR-1G was maximally expressed (- Doxy)(Table 2), which was consistent with the B_{max} value increase seen in saturation studies with [^{3}H]DAMGO. In the Tet-off

Molecular Pharmacology Fast Forward. Published on July 28, 2020 as DOI: 10.1124/mol.120.119453
This article has not been copyedited and formatted. The final version may differ from this version.

CHO cell line expressing only mMOR-1G without expression of 7TM mMOR-1, [^{35}S]GTPγS binding with mu agonists, including DAMGO, morphine and lBNtxA, showed no G-protein stimulation (Fig. S3). Thus, the mu agonist-induced G protein stimulation seen in the Tet-off CHO cell line co-expressing 7TM mMOR-1 and 6TM mMOR-1G is mediated through 7TM mMOR-1. Together, these results suggest that 6TM mMOR-1G does not change mRNA expression of 7TM mMOR-1, but enhances expression of functional 7TM mMOR-1 at the protein level.

To further confirm that mMOR-1G can increase expression of the 7TM mMOR-1 at the protein level, we used an immunoprecipitation (IP) approach in an *OPRM1*-Knockdown (KD) Be(2)C cell line transiently transfected with Flag-tagged mMOR-1 (mMOR-1/Flag) or HA-tagged mMOR-1G (mMOR-1G/HA), or both mMOR-1/Flag and mMOR-1G/HA. When compared to transfection with mMOR-1/Flag alone, co-transfection of both mMOR-1/Flag and mMOR-1G/HA significantly increased mMOR-1/Flag level in both immunoblots (Figs. 2A, 2B, 3A & 3B) and [^{3}H]DAMGO binding (Fig. 3C), which was consistent with the results seen in the Tet-Off cells with non-tagged constructs.

We next performed [^{3}H]DAMGO competition assays with several opioids to investigate whether the co-expression of mMOR-1 with mMOR-1G can modulate mu binding selectivity and affinity in the Tet-Off CHO cells. When mMOR-1G was not present (+Doxy), mu drugs such as morphine, DAMGO, fentanyl, and M6G all competed binding quite potently, whereas kappa drug U50,488H and delta drug DPDPE were both ineffective (Table 1). Co-expression of mMOR-1G (-Doxy) did not alter the K_i values of most drugs, demonstrating that co-expressing mMOR-1G does not affect their

Molecular Pharmacology Fast Forward. Published on July 28, 2020 as DOI: 10.1124/mol.120.119453
This article has not been copyedited and formatted. The final version may differ from this version.

binding affinity or selectivity for mMOR-1 (Table 1). However, co-expressing mMOR-1G led to a small, but significant decrease of the K_i values for M6G and β-endorphin, which raises the interesting question of whether mMOR-1G co-expression has a structural impact on the binding pocket of mMOR-1.

6TM variant mMOR-1G increases 7TM mMOR-1 receptor levels at the plasma membrane in a Tet-Off CHO cell line

We next defined the subcellular distribution of the 7TM mMOR-1 expression in the Tet-Off CHO cells treated with 100 ng/ml of doxycycline (+Doxy, no mMOR-1G expression) or without doxycycline (-Doxy, mMOR-1G co-expression) via subcellular fractionation analysis using OptiPrep density gradient centrifugation, a common method for separating subcellular organelle membranes. The post-nuclear supernatants were resolved by centrifugation through OptiPrep gradients (2 – 26%) and collected from the top in fourteen fractions that showed a near linear OptiPrep density from 1.00 – 1.25 g/ml (Fig. 4A). Western blot analysis with the organelle marker antibodies revealed that the plasma membrane indicated by N-Cadherin bands were enriched in fractions 7 - 8, whereas the ER membrane shown by the calnexin bands were peaked in fractions 10 - 11 (Figs. 4B & 4C). Similar results were obtained using Na+,K+-ATPase antibody, another plasma membrane marker, and calreticulin antibody, another ER marker (data not shown). Although slightly overlapping, the peaks of these two markers were adequately separated.

We then determined the expression of the functional 7TM mMOR-1 receptor in each collected fraction using [^{3}H]DAMGO binding. The peak of [^{3}H]DAMGO binding in

Molecular Pharmacology Fast Forward. Published on July 28, 2020 as DOI: 10.1124/mol.120.119453
This article has not been copyedited and formatted. The final version may differ from this version.

either +Doxy or –Doxy cells overlapped well with plasma membrane-enriched fractions (Fig. 4A), suggesting that functional and mature mMOR-1 was expressed mainly in the plasma membrane. Furthermore, we demonstrated a significant increase of [^{3}H]DAMGO binding in –Doxy cells (mMOR-1G co-expression) compared to +Doxy cells (no mMOR-1G expression) in plasma membrane-enriched fractions (Fig. 4A). These data illustrate that an increased expression of the functional 7TM mMOR-1 via mMOR-1G co-expression also occurs mainly in the plasma membrane.

Physical association of 6TM variant mMOR-1G with 7TM mMOR-1

Enhanced expression of mMOR-1 protein by co-expression of mMOR-1G in the Tet-Off cell line raised the question of whether 6TM mMOR-1G can physically associate with 7TM mMOR-1. We addressed this question by performing co-immunoprecipitation (Co-IP) assays in the *OPRM1*-Knockdown (KD) Be(2)C cells transiently co-transfected with Flag-tagged mMOR-1 (mMOR-1/Flag) and HA-tagged mMOR-1G (mMOR-1G/HA) constructs. We observed that mMOR-1/Flag was detected with anti-Flag antibody in the IP elution using anti-HA antibody-conjugated beads from the co-transfections (Fig. 2A, Lane 1 in the third panel). The converse Co-IP experiment also detected mMOR-1G/HA with anti-HA antibody in the IP elution using anti-Flag antibody-conjugated beads from the co-transfection (Fig. 2A, Lane 1 in the fourth panel). The specificity of the physical association was confirmed by parallel IP using cells transfected with mMOR-1/Flag or mMOR-1G/HA alone (Fig. 2A, Lanes 2 & 3 in the third and fourth panels, respectively). Together, these results indicate physical association or heterodimerization between mMOR-1G/HA and mMOR-1/Flag. The mMOR-1/Flag bands were shown with wide-

Molecular Pharmacology Fast Forward. Published on July 28, 2020 as DOI: 10.1124/mol.120.119453
This article has not been copyedited and formatted. The final version may differ from this version.

range of molecular weights from 50 – 90 kDa, most likely due to differential glycosylation of the receptor, which was consistent with those reported from literature. Only monomer mMOR-1/Flag or mMOR-1G/HA with their predicted molecular weights were shown on immunoblots, suggesting that they physically associated or heterodimerized during IP, but dissociated in the presence SDS in the SDS-PAGE. Furthermore, co-transfection of mMOR-1/Flag with mMOR-1G/HA significantly increased immunoprecipitated mMOR-1/Flag protein compared to transfection of mMOR-1/Flag alone (Fig. 2A, the top panel). Since the same amount of mMOR-1/Flag plasmid DNA was used in the transfection and the same amount of cells was used in IP and IB, these results suggest that mMOR-1G/HA can increase expression of mMOR-1/Flag at the protein level, which was consistent with the increase of [^{3}H]DAMGO and [^{35}S]GTPγS binding seen in the Tet-Off cell line co-expressing mMOR-1 and mMOR-1G.

Since Co-IP was performed using lysates from whole cells, the subcellular compartment location of dimerization between mMOR-1/Flag and mMOR-1G/HA was unknown. To determine location of dimerization, we transfected cells treated with or without Brefeldin A (BFA). BFA blocks protein transport from the endoplasmic reticulum (ER) to the Golgi, resulting an accumulation of proteins in the ER and preventing further protein maturation in the Golgi. If dimerization occurs in compartments downstream from the ER, we would expect to see no dimerization after BFA treatment. The Co-IP experiment revealed that the dimerization between mMOR-1/Flag and mMOR-1G/HA was preserved in BFA treated cells (Fig. 3A, Lanes 1 and 3 in the second and third panels), suggesting that this dimerization occurs within the ER. BFA treated cells

Molecular Pharmacology Fast Forward. Published on July 28, 2020 as DOI: 10.1124/mol.120.119453
This article has not been copyedited and formatted. The final version may differ from this version.

showed the same increase in expression level of mMOR-1/Flag protein by co-expression of mMOR-1G/HA, as indicated by immunoblot (Figs. 3A & 3B), implying that dimerization within the ER leads to the increased expression of the full-length 7TM Flag-mMOR-1 protein at the plasma membrane.

Additionally, BFA treatment led to a loss of mMOR-1/Flag proteins with higher molecular weights (~ 70 – 90 kDa) as shown on immunoblots (Fig. 3A, Lanes 3 & 4 in the first and second panels), suggesting that BFA eliminates further glycosylation or maturation of the mMOR-1/Flag, most likely in the Golgi. This downstream glycosylation or maturation appears to be crucial in producing a functional receptor. BFA treatment abolished almost all [^{3}H]DAMGO binding in either co-transfection or single mMOR-1/Flag transfection (Fig. 3C), despite the fact that the mMOR-1/Flag proteins with the lower molecular weight (~ 50 – 70 kDa) were present (Fig. 3A, Lanes 3 & 4 in the first panel).

Molecular Pharmacology Fast Forward. Published on July 28, 2020 as DOI: 10.1124/mol.120.119453
This article has not been copyedited and formatted. The final version may differ from this version.

Discussion

In the present study, we demonstrate a novel role of the *Oprm1* 6TM variant, mMOR-1G, in enhancing expression of the 7TM mMOR-1 at the protein level. This conclusion was based on the results from [^{3}H]DAMGO and [^{35}S]GTPγS binding assays in a Tet-Off CHO cell system, as well as immunoprecipitation and Western blot analysis in an *OPRM1*-KD Be(2)C cell line transiently transfected with tagged mMOR-1 and mMOR-1G constructs. Using a Co-IP approach, we further demonstrate that mMOR-1G physically associates with the 7TM mMOR-1 starting at the ER, contributing to the enhanced expression of 7TM mMOR-1 protein at the plasma membrane. The physical association of mMOR-1G does not modify the binding affinity of mMOR-1 in saturation studies, as the K_D values remain unchanged, but increases mMOR-1 receptor levels, shown by an increase in B_{max} values in saturation study and an increase of % stimulation in [^{35}S]GTPγS binding assays in the Tet-Off cells co-expressing mMOR-1 and mMOR-1G.

Increased expression of 7TM mMOR-1 protein with co-expression of 6TM mMOR-1G is not correlated with mMOR-1 mRNA levels. Instead, immunoprecipitation and Western blot analysis show an increase of 7TM mMOR-1/Flag protein levels, which corresponds to the increased B_{max} in saturation study and % stimulation in [^{35}S]GTPγS binding studies. Our earlier studies showed that *Oprm1* single TM variants dimerize with 7TM mMOR-1 in the ER, leading to increased 7TM mMOR-1 protein expression via chaperone-like function (Xu et al., 2013). Like the single TM variants, 6TM mMOR-1G can dimerize with 7TM mMOR-1 and increase its protein expression in the ER shown by the BFA treatment studies. Our data suggest that 6TM mMOR-1G increases expression

Molecular Pharmacology Fast Forward. Published on July 28, 2020 as DOI: 10.1124/mol.120.119453
This article has not been copyedited and formatted. The final version may differ from this version.

of mMOR-1 through a chaperone-like mechanism similar to what is seen with the single TM variants. The observation that increased mMOR-1 was mainly distributed at the plasma membrane-enriched fractions by subcellular fractionation analysis further supports the chaperone-like role of the 6TM mMOR-1G. This chaperone-like mechanism is also observed in the actions of several opioid agonists and antagonists (Chaipatikul et al., 2003a; Chaipatikul et al., 2003b; Chen et al., 2006; Leskela et al., 2007; Wannemacher et al., 2007).

The physical association between mMOR-1G with mMOR-1 does not alter the binding affinity for morphine, DAMGO and fentanyl in competition assays. However, it significantly improves the binding affinity for M6G and β-endorphin by lowing their respective K_i values. Interestingly, the improved binding affinity for M6G and β-endorphin by mMOR-1/mMOR-1G dimerization was not seen in the dimerization of the single TM variants with mMOR-1 (Xu et al., 2013). This suggests that the association of mMOR-1G with mMOR-1 may slightly alter the agonist conformation of the 7TM mMOR-1, favoring binding to M6G and β-endorphin, while association with the single TM variants does not have similar structural changes. It will be interesting to explore these structural changes of mMOR-1/mMOR-1G dimerization using computer simulation models or crystal structures in the future.

Unlike detergent-resistant heterodimerization between DOR-1 and KOR-1 (Jordan and Devi, 1999), the heterodimerization between mMOR-1G and mMOR-1 was not stable in SDS PAGE since only the monomers were observed on immunoblots. The crystal structure of mMOR-1 revealed that the mMOR-1 homodimer was formed mainly through TM5 and TM6 (Manglik et al., 2012). Although both mMOR-1 and mMOR-1G

Molecular Pharmacology Fast Forward. Published on July 28, 2020 as DOI: 10.1124/mol.120.119453
This article has not been copyedited and formatted. The final version may differ from this version.

have the same TM domains from TM2 to TM7, the detergent-sensitive interaction between mMOR-1 and mMOR-1G raises questions of whether TM5 and TM6 are the regions responsible for mMOR-1/mMOR-1G heterodimerization or whether additional regions are involved.

The current study only focused on mMOR-1G, one of five 6TM variants in mouse, raising the question of whether other 6TM variants have a similar chaperone-like function. All five 6TM variants share the same TM2 to TM7 and part of intracellular C-terminal sequence encoded by exon 3, but have different N-termini or C-termini generated by alternative 5' or 3' splicing, respectively (Pan et al., 2001b). We have preliminary data to indicate that two other 6TM variants, mMOR-1M and mMOR-1N, can also physically associate with mMOR-1 (data not shown), implying that they can enhance 7TM mMOR-1 expression at the protein level through a similar mechanism as mMOR-1G. These data need to be verified in future studies.

N-terminal glycosylation has been shown to be important for expression of functional MOR-1. [^{3}H]funaltrexamine labeling studies (Liu-Chen et al., 1993) and Western blot analyses using N-glycanase (Huang et al., 2008; Huang and Liu-Chen, 2009) demonstrate that 7TM MOR-1 is heavily glycosylated at the N-terminus. A single nucleotide polymorphism (SNP), A118G, located at a N-glycosylation site of the human MOR-1, was shown to alter β-endorphin binding (Bond et al., 1998; Kroslak et al., 2007), and modulate expression of MOR-1 mRNA and protein (Zhang et al., 2005). An A112G mutation which mimics human SNP, A118G, in mouse altered MOR-1 glycosylation and modulated MOR-1 stability at the protein level (Huang et al., 2012).

Molecular Pharmacology Fast Forward. Published on July 28, 2020 as DOI: 10.1124/mol.120.119453
This article has not been copyedited and formatted. The final version may differ from this version.

Our BFA study further suggests that MOR-1 glycosylation is essential for maturation and function of the 7TM mu opioid receptor.

Multiple *Oprm1* full-length 7TM variants have been identified, which all contain identical receptor protein structures, and differ only at the tip of the intracellular C-terminus. The current study focused on mMOR-1, one of the most dominant and abundant C-terminal variants. It is likely that 6TM variants can dimerize with other full-length 7TM C-terminal variants since they share the same TM domains, if the TM regions, particularly TM5 and TM6 that are responsible for MOR-1 homodimer (Manglik et al., 2012), are the main regions involved in dimerization.

Using *in vivo Oprm1* gene targeting mouse models, we have previously shown that the 6TM variants are essential targets for a novel class of opioids such as IBNtxA (Lu et al., 2015; Lu et al., 2018; Majumdar et al., 2011b). They are also implicated in analgesic actions of delta and kappa drugs, as well as non-opioid drugs such as clonidine, an α_2-adrenergic agonist (Marrone et al., 2016). However, when expressed in cell lines alone, the 6TM variants do not bind to any known opioids, raising questions regarding the molecular mechanisms underlying their *in vivo* functions. One hypothesis is that the *in vivo* actions of the 6TM variants are mediated through their physical association with a GPCR or non-GPCR protein. [^{125}I]IBNtxA bound to a site in a triple KO mouse brain, which was similar to that in wide-type mouse brain in the present of the mu-delta-kappa blockers (Majumdar et al., 2011b). IBNtxA analgesia in the triple KO was also normal. In the triple KO mouse, all opioid receptors including the 7TM mu opioid receptors, DOR-1 and KOR-1 were disrupted, but expression of the 6TM variants was preserved. We speculate that 6TM variants interact with other receptors or non-

Molecular Pharmacology Fast Forward. Published on July 28, 2020 as DOI: 10.1124/mol.120.119453
This article has not been copyedited and formatted. The final version may differ from this version.

receptor proteins constitute the [^{125}I]IBNtxA binding site and produce IBNtxA analgesia observed in the triple KO mice. Co-expression of mMOR-1G and ORL1 receptor in HEK293 cells reconstituted [^{125}I]IBNtxA binding, suggesting heterodimerization between these two receptors (Majumdar et al., 2011b). However, it remains unknown whether the interaction of mMOR-1G with ORL-1 corresponds to IBNtxA analgesia in mice. Future studies should explore the action of IBNtxA in ORL-1 KO or E1/ORL-1 double KO or Quad KO (the triple KO plus ORL-1 KO). The 6TM variants can also heterodimerize with β_2-adrenoreceptor, leading to synergistic analgesia when the 6TM and β_2-adrenoreceptor drugs were co-administered (Samoshkin et al., 2015). The current study provides another example of the physical association between 6TM mMOR-1G and 7TM mMOR-1 at least *in vitro*. However, their *in vivo* physical interaction and related functions need further exploration.

Eliminating 6TM variants in an E11-KO mouse led to loss of IBNtxA analgesia but did not affect morphine analgesia (Majumdar et al., 2011b). Knocking out all the 7TM variants in an E1-KO or a triple KO mouse resulted in loss of morphine analgesia, but preserved IBNtxA analgesia (Pasternak and Pan, 2013; Schuller et al., 1999). Thus, the potential association between the 6TM and 7TM variants *in vivo* cannot contribute to either morphine or IBNtxA analgesia. However, increasing evidence suggests that the 6TM variants are involved in several other actions of morphine. The loss of 6TM variants in the E11-KO mice led to reduction of morphine tolerance, hyperalgesia and locomotor activity (Marrone et al., 2017). mMOR-1K, another mouse 6TM variant, has been implicated in morphine hyperalgesia (Gris et al., 2010; Oladosu et al., 2015). Our study raises intriguing questions of whether the roles of the 6TM variants in these

Molecular Pharmacology Fast Forward. Published on July 28, 2020 as DOI: 10.1124/mol.120.119453
This article has not been copyedited and formatted. The final version may differ from this version.

morphine actions are mediated through the physical association between 6TM and 7TM variants *in vivo*.

Truncated 6TM variants are not limited to the *OPRM1* gene. Approximately 6% of human GPCR genes (excluding olfactory receptor genes) have predicted 6TM splice variants based on genomic database analysis (unpublished observation). The current study opens avenues of inquiry as to whether other 6TM variants may have a similar function in enhancing 7TM receptor expression.

In summary, the current study illustrates that the 6TM mMOR-1G enhances expression of the functional 7TM mMOR-1 at the protein level. mMOR-1G physically interacts with mMOR-1 starting at the ER, enhancing mMOR-1 expression at the plasma membrane through a chaperone-like function. Our study also raises questions for future exploration of the functional relevance of *Oprm1* 6TM/7TM interactions *in vivo*.

Molecular Pharmacology Fast Forward. Published on July 28, 2020 as DOI: 10.1124/mol.120.119453
This article has not been copyedited and formatted. The final version may differ from this version.

Authorship Contributions:

Participated in research design: Zhang, Xu and Pan.

Conducted experiments: Zhang, Xu and Pan.

Contributed new reagents or analytic tools: Zhang and Pan.

Performed data analysis: Zhang, Xu and Pan.

Wrote or contributed to the writing of the manuscript: Zhang and Pan.

Molecular Pharmacology Fast Forward. Published on July 28, 2020 as DOI: 10.1124/mol.120.119453
This article has not been copyedited and formatted. The final version may differ from this version.

References

Abbadie C, Gultekin SH and Pasternak GW (2000a) Immunohistochemical localization of the carboxy terminus of the novel mu opioid receptor splice variant MOR-1C within the human spinal cord. *Neuroreport* **11**:1953-1957.

Abbadie C, Pan YX, Drake CT and Pasternak GW (2000b) Comparative immunohistochemical distributions of carboxy terminus epitopes from the mu-opioid receptor splice variants MOR-1D, MOR-1 and MOR-1C in the mouse and rat CNS. *Neuroscience* **100**:141-153.

Abbadie C, Pan YX and Pasternak GW (2004) Immunohistochemical study of the expression of exon11-containing mu opioid receptor variants in mouse brain. *Neuroscience* **127**:419-430.

Bolan EA, Pan Y-X and Pasternak GW (2000) Functional characterization of several alternatively spliced mu opioid receptor (MOR-1) isoforms. *SocNeurosci* **26**:112.

Bond C, LaForge KS, Tian M, Melia D, Zhang S, Borg L, Gong J, Schluger J, Strong JA, Leal SM, Tischfield JA, Kreek MJ and Yu L (1998) Single-nucleotide polymorphism in the human mu opioid receptor gene alters beta-endorphin binding and activity: possible implications for opiate addiction. *ProcNatlAcad Sci USA* **95**:9608-9613.

Caron MG, Bohn LM, Barak LS, Abbadie C, Pan Y-X and Pasternak GW (2000) Mu opioid receptor spliced variant, MOR1D, internalizes after morphine treatment in HEK-293 cells. *SocNeurosci* **26**:783.783.

Chaipatikul V, Erickson-Herbrandson LJ, Loh HH and Law PY (2003a) Rescuing the traffic-deficient mutants of rat mu-opioid receptors with hydrophobic ligands. *Molecular pharmacology* **64**:32-41.

Chaipatikul V, Loh HH and Law PY (2003b) Ligand-Selective Activation of {micro}-Opioid Receptor: Demonstrated with Deletion and Single Amino Acid Mutations of Third Intracellular Loop Domain. *Journal of Pharmacology and Experimental Therapeutics* **305**:909-918.

Chen Y, Chen C, Wang Y and Liu-Chen LY (2006) Ligands regulate cell surface level of the human kappa opioid receptor by activation-induced down-regulation and pharmacological chaperone-mediated enhancement: differential effects of nonpeptide and peptide agonists. *The Journal of pharmacology and experimental therapeutics* **319**:765-775.

Gris P, Gauthier J, Cheng P, Gibson DG, Gris D, Laur O, Pierson J, Wentworth S, Nackley AG, Maixner W and Diatchenko L (2010) A novel alternatively spliced isoform of the mu-opioid receptor: functional antagonism. *Mol Pain* **6**:33.

Huang P, Chen C, Mague SD, Blendy JA and Liu-Chen LY (2012) A common single nucleotide polymorphism A118G of the mu opioid receptor alters its N-glycosylation and protein stability. *Biochem J* **441**:379-386.

Huang P, Chen C, Xu W, Yoon SI, Unterwald EM, Pintar JE, Wang Y, Chong PL and Liu-Chen LY (2008) Brain region-specific N-glycosylation and lipid rafts association of the rat mu opioid receptor. *BiochemBiophysResCommun* **365**:82-88.

Molecular Pharmacology Fast Forward. Published on July 28, 2020 as DOI: 10.1124/mol.120.119453
This article has not been copyedited and formatted. The final version may differ from this version.

Huang P and Liu-Chen LY (2009) Detection of the endogenous mu opioid receptor (mopr) in brain. *Front Biosci* **1**:220-227.

Jordan BA and Devi LA (1999) G-protein-coupled receptor heterodimerization modulates receptor function. *Nature* **399**:697-700.

Koch T, Schulz S, Pfeiffer M, Klutzny M, Schroder H, Kahl E and Hollt V (2001) C-terminal splice variants of the mouse mu-opioid receptor differ in morphine-induced internalization and receptor resensitization. *JBiolChem* **276**:31408-31414.

Koch T, Schulz S, Schroder H, Wolf R, Raulf E and Hollt V (1998) Carboxyl-terminal splicing of the rat mu opioid receptor modulates agonist-mediated internalization and receptor resensitization. *J BiolChem* **273**:13652-13657.

Kroslak T, LaForge KS, Gianotti RJ, Ho A, Nielsen DA and Kreek MJ (2007) The single nucleotide polymorphism A118G alters functional properties of the human mu opioid receptor. *J Neurochem* **103**:77-87.

Leskela TT, Markkanen PM, Pietila EM, Tuusa JT and Petaja-Repo UE (2007) Opioid receptor pharmacological chaperones act by binding and stabilizing newly synthesized receptors in the endoplasmic reticulum. *The Journal of biological chemistry* **282**:23171-23183.

Liu-Chen L-Y, Chen C and Phillips CA (1993) b-[^{3}H]Funaltrexamine-labeled m-opioid receptors: Species variations in molecular mass and glycosylation by complex-type, *N*-linked oligosaccharides. *MolPharmacol* **44**:749-756.

Lu Z, Xu J, Rossi GC, Majumdar S, Pasternak GW and Pan YX (2015) Mediation of opioid analgesia by a truncated 6-transmembrane GPCR. *The Journal of clinical investigation* **125**:2626-2630.

Lu Z, Xu J, Xu M, Rossi GC, Majumdar S, Pasternak GW and Pan YX (2018) Truncated mu-Opioid Receptors With 6 Transmembrane Domains Are Essential for Opioid Analgesia. *Anesthesia and analgesia* **126**:1050-1057.

Majumdar S, Burgman M, Haselton N, Grinnell S, Ocampo J, Pasternak AR and Pasternak GW (2011a) Generation of novel radiolabeled opiates through site-selective iodination. *BioorgMed Chem Lett* **21**:4001-4004.

Majumdar S, Grinnell S, Le R, V, Burgman M, Polikar L, Ansonoff M, Pintar J, Pan YX and Pasternak GW (2011b) Truncated G protein-coupled mu opioid receptor MOR-1 splice variants are targets for highly potent opioid analgesics lacking side effects. *Proceedings of the National Academy of Sciences of the United States of America* **108**:19778-19783.

Majumdar S, Subrath J, Le R, V, Polikar L, Burgman M, Nagakura K, Ocampo J, Haselton N, Pasternak AR, Grinnell S, Pan YX and Pasternak GW (2012) Synthesis and Evaluation of Aryl-Naloxamide Opiate Analgesics Targeting Truncated Exon 11-Associated mu Opioid Receptor (MOR-1) Splice Variants. *J Med Chem* **55**:6352-6362.

Manglik A, Kruse AC, Kobilka TS, Thian FS, Mathiesen JM, Sunahara RK, Pardo L, Weis WI, Kobilka BK and Granier S (2012) Crystal structure of the mu-opioid receptor bound to a morphinan antagonist. *Nature* **485**:321-U170.

Marrone GF, Grinnell SG, Lu Z, Rossi GC, Le Rouzic V, Xu J, Majumdar S, Pan YX and Pasternak GW (2016) Truncated mu opioid GPCR variant involvement in opioid-dependent and opioid-independent pain modulatory systems within the CNS. *Proceedings of the National Academy of Sciences of the United States of America* **113**:3663-3668.

Marrone GF, Le Rouzic V, Varadi A, Xu J, Rajadhyaksha AM, Majumdar S, Pan YX and Pasternak GW (2017) Genetic dissociation of morphine analgesia from hyperalgesia in mice. *Psychopharmacology* **234**:1891-1900.

Oladosu FA, Conrad MS, O'Buckley SC, Rashid NU, Slade GD and Nackley AG (2015) Mu Opioid Splice Variant MOR-1K Contributes to the Development of Opioid-Induced Hyperalgesia. *PloS one* **10**:e0135711.

Pan L, Xu J, Yu R, Xu MM, Pan YX and Pasternak GW (2005) Identification and characterization of six new alternatively spliced variants of the human mu opioid receptor gene, Oprm. *Neuroscience* **133**:209-220.

Pan Y-X, Xu J, Mahurter L, Bolan EA, Xu MM and Pasternak GW (2001a) Generation of the mu opioid receptor (MOR-1) protein by three new splice variants of the *Oprm* gene. *ProcNatlAcadSciUSA* **98**:14084-14089.

Pan YX (2005) Diversity and complexity of the mu opioid receptor gene: alternative pre-mRNA splicing and promoters. *DNA Cell Biol* **24**:736-750.

Pan YX, Xu A, Mahurter L, Bolan E, Xu MM and Pasternak GW (2001b) Generation of the mu opioid receptor (MOR-1) protein by three new splice variants of the Oprm gene. *Proceedings of the National Academy of Sciences of the United States of America* **98**:14084-14089.

Pan YX, Xu J, Bolan EA, Abbadie C, Chang A, Zuckerman A, Rossi GC and Pasternak GW (1999) Identification and characterization of three new alternatively spliced mu opioid receptor isoforms. *MolPharmacol* **56**:396-403.

Pasternak GW and Pan YX (2013) Mu opioids and their receptors: evolution of a concept. *Pharmacological reviews* **65**:1257-1317.

Samoshkin A, Convertino M, Viet CT, Wieskopf JS, Kambur O, Marcovitz J, Patel P, Stone LS, Kalso E, Mogil JS, Schmidt BL, Maixner W, Dokholyan NV and Diatchenko L (2015) Structural and functional interactions between six-transmembrane mu-opioid receptors and beta2-adrenoreceptors modulate opioid signaling. *Scientific reports* **5**:18198.

Schuller AG, King MA, Zhang J, Bolan E, Pan YX, Morgan DJ, Chang A, Czick ME, Unterwald EM, Pasternak GW and Pintar JE (1999) Retention of heroin and morphine-6 beta-glucuronide analgesia in a new line of mice lacking exon 1 of MOR-1. *NatNeurosci* **2**:151-156.

Tanowitz M, Hislop JN and von ZM (2008) Alternative splicing determines the post-endocytic sorting fate of G-protein-coupled receptors. *JBiolChem* **283**:35614-35621.

Wannemacher KM, Yadav PN and Howells RD (2007) A select set of opioid ligands induce up-regulation by promoting the maturation and stability of the rat kappa-opioid receptor in human embryonic kidney 293 cells. *The Journal of pharmacology and experimental therapeutics* **323**:614-625.

Wieskopf JS, Pan YX, Marcovitz J, Tuttle AH, Majumdar S, Pidakala J, Pasternak GW and Mogil JS (2014) Broad-spectrum analgesic efficacy of IBNtxA is mediated by

exon 11-associated splice variants of the mu-opioid receptor gene. *Pain* **155**:2063-2070.

Xu J, Lu Z, Narayan A, Le Rouzic VP, Xu M, Hunkele A, Brown TG, Hoefer WF, Rossi GC, Rice RC, Martinez-Rivera A, Rajadhyaksha AM, Cartegni L, Bassoni DL, Pasternak GW and Pan YX (2017) Alternatively spliced mu opioid receptor C termini impact the diverse actions of morphine. *The Journal of clinical investigation* **127**:1561-1573.

Xu J, Lu Z, Xu M, Rossi GC, Kest B, Waxman AR, Pasternak GW and Pan YX (2014) Differential expressions of the alternatively spliced variant mRNAs of the micro opioid receptor gene, OPRM1, in brain regions of four inbred mouse strains. *PloS one* **9**:e111267.

Xu J, Xu M, Brown T, Rossi GC, Hurd YL, Inturrisi CE, Pasternak GW and Pan YX (2013) Stabilization of the mu-opioid receptor by truncated single transmembrane splice variants through a chaperone-like action. *The Journal of biological chemistry* **288**:21211-21227.

Zhang Y, Wang D, Johnson AD, Papp AC and Sadee W (2005) Allelic Expression Imbalance of Human mu Opioid Receptor (OPRM1) Caused by Variant A118G. *Journal of Biological Chemistry* **280**:32618-32624.

Molecular Pharmacology Fast Forward. Published on July 28, 2020 as DOI: 10.1124/mol.120.119453
This article has not been copyedited and formatted. The final version may differ from this version.

Footnotes:

This work was supported by grants from the National Institute on Drug Abuse of the National Institutes of Health (DA06241, DA07242, DA042888, DA040858 and DA046714), the Mayday Foundation and the Peter F. McManus Charitable Trust to YXP, and a core grant from the National Cancer Institute (CA008748) to Memorial Sloan Kettering Cancer Center.

Molecular Pharmacology Fast Forward. Published on July 28, 2020 as DOI: 10.1124/mol.120.119453
This article has not been copyedited and formatted. The final version may differ from this version.

Figure Legends:

Fig. 1. Enhanced functional mMOR-1 protein expression by mMOR-1G co-expression in Tet-Off CHO cells.

A: [^{3}H]DAMGO binding (n = 3). [^{3}H]DAMGO binding was performed using membranes isolated from a Tet-Off cell line with constitutive expression of mMOR-1 and doxycycline (Doxy)-regulated mMOR-1G in the presence or absence of the indicated concentration of Doxy, as described in Materials and Methods. mMOR-1G expression was controlled by doxycycline so the highest expression level of mMOR-1G was seen in the absence of doxycycline. Increasing concentrations of doxycycline resulted in progressively reduced levels of mMOR-1G expression. *Triangle* shows the expression levels of mMOR-1G.

B and C: Expression of mMOR-1 (*B, n =3*) and mMOR-1G (*C, n = 3*) mRNAs. Total RNAs isolated from the same Tet-Off cells were used for RT-qPCR as described in Materials and Methods. G3PDH and m18S were used for normalization. Expression levels were calculated through $2^{-(\Delta C(t))}$ and normalized using the samples from the Tet-Off cells with doxycycline (100 ng), which is set as 100%. All significant differences were analyzed by one-way ANOVA with *post hoc* Bonferroni's multiple comparisons test. *: $p < 0.05$; ***: $p < 0.001$; ****: $p < 0.0001$.

Fig. 2. Increased mMOR-1/Flag protein expression by mMOR-1G/HA co-expression through their heterodimerization in *OPRM1*-KD Be(2)C cells

A: Co-IP study (n = 3). The transient transfection, solubilization and immunoprecipitation/immunoblot were performed as described in Materials and

Molecular Pharmacology Fast Forward. Published on July 28, 2020 as DOI: 10.1124/mol.120.119453
This article has not been copyedited and formatted. The final version may differ from this version.

Methods. Equal amounts of mMOR-1/Flag and mMOR-1/HA plasmid DNAs were used in transient co-transfection (Lane 1). The amount of mMOR-1/Flag or mMOR-1G/HA in single transfection (Lanes 2 or 3) was same as the co-transfection, but pcDNA3.1 DNA was included to keep the total amount of DNA constant in all transfections. ***Top panel:*** immunoblots (IB) with the Flag antibody on the elution fractions immunoprecipitated with EZview Red Anti-Flag (M2) beads; ***The second panel from the top***, immunoblots with the HA antibody on the elution fractions immunoprecipitated with EZview Red Anti-HA beads; ***The third panel from the top***, immunoblots with the Flag antibody on the elution fractions immunoprecipitated with EZview Red Anti-HA beads. ***The fourth panel from the top***, immunoblots with the HA antibody on the elution fractions immunoprecipitated with EZview Red Anti-Flag (M2) beads. ***Bottom panel***, immunoblots with GAPDH antibody on lysates used for immunoprecipitation.
B: Quantification of mMOR-1/Flag in the top panel of A (n = 3). The band intensities were analyzed by using Image Lab software (Bio-Rad). The expression level of mMOR-1/Flag was calculated by normalizing mMOR-1/Flag level as the mMOR-1/Flag/GAPDH ratio with the bands from transfected with mMOR-1G/HA (Lane 3). Significant difference was calculated by using one-way ANOVA with *post hoc* Bonferroni's multiple comparisons test. **: $p < 0.01$; ***: $p < 0.001$.

Fig. 3. Effect of Brefeldin A on expression of mMOR-1/Flag induced by mMOR-1G/HA and heterodimerization of mMOR-1/Flag and mMOR-1G/HA in *OPRM1*-KD Be(2)C cells
A: Co-IP study (n = 3). The transient transfection, brefeldin A (BFA) treatment, solubilization and immunoprecipitation/immunoblot were performed as described in

Molecular Pharmacology Fast Forward. Published on July 28, 2020 as DOI: 10.1124/mol.120.119453
This article has not been copyedited and formatted. The final version may differ from this version.

Materials and Methods. Again, equal amounts of mMOR-1/Flag and mMOR-1G/HA plasmid DNAs were used for co-transfection (Lanes 1 and 3). The amount of mMOR-1/Flag in single transfection (Lanes 2 and 4) was same as the co-transfection (Lanes 1 and 3), but pcDNA3.1 was added to keep the total amount of DNAs constant. Eight hours after transfection, the cells were treated with or without 4 μg/ml of BFA for additional 24 hours before harvesting. ***Top panel***, immunoblots (IB) with the Flag antibody on the elution fractions immunoprecipitated with EZview Red Anti-Flag (M2) beads; ***The second panel from the top***, immunoblots with the Flag antibody on the elution fractions immunoprecipitated with EZview Red Anti-HA beads; ***The third panel from the top***, immunoblots with the HA antibody on the elution fractions immunoprecipitated with EZview Red Anti-Flag (M2) beads. ***Bottom panel***, immunoblots with a GAPDH antibody on lysates used for immunoprecipitation.
B: Quantification of immunoblots in A ($n = 3$). Band intensities were analyzed using Image Lab software (Bio-Rad). Significant difference was calculated by one-way ANOVA with *post hoc* Bonferroni's multiple comparisons test. *: $p < 0.05$; **: $p < 0.01$.
C: [^{3}H]DAMGO binding using membranes isolated from cells with indicated constructs and BFA treatment ($n = 3$). Significant difference was calculated by one-way ANOVA with *post hoc* Bonferroni's multiple comparisons test. *: $p < 0.05$; ****, $p < 0.0001$.

Fig. 4. Increased expression of the functional mMOR-1 by mMOR-1G in the Tet-Off cells at the plasma membrane-enriched fractions
A: Subcellular fractionation analysis. The Tet-Off cells co-expressing mMOR-1 and mMOR-1G were treated with 100 ng/ml of doxycycline (+ Doxy) and without doxycycline

Molecular Pharmacology Fast Forward. Published on July 28, 2020 as DOI: 10.1124/mol.120.119453
This article has not been copyedited and formatted. The final version may differ from this version.

(- Doxy), homogenized and fractionated in OptiPrep density gradient (2 -26%) through ultracentrifugation, as described in Materials and Methods. OptiPrep density of each fraction was determined by measuring absorbance 340 nm following the manufacturer's instructions (Axis-Shield). 125 µl/tube of each fraction was used in [^{3}H]DAMGO (1.5 nM) binding as described in Materials and Methods. Specific binding was calculated by subtracting total binding with nonspecific binding at the presence of 10 µM levallorphan. Data represented the means ± SD of three experiments. Significant difference was calculated by two-way ANOVA with *post hoc* Bonferroni's multiple comparisons test. Compared to – Doxy, **: $p < 0.01$; ***, $p < 0.001$.

B: Western blot analysis. Equal volume of samples from each fraction was treated with SDS sample buffer, separated on Any kD SDS-PAGE and transferred onto PVDF membrane, as described in Materials and Methods. The PVDF membranes were used in immunoblot with anti-N-Cadherine antibody (1:1800, Novus Biologicals), a plasma membrane marker or anti-calnexin antibody (1:2000, Novus Biologicals), an ER marker, as described in Materials and Methods.

C: Quantification of Western blots in Fig. 4B ($n = 3$). The band intensities were analyzed by using Image Lab software (Bio-Rad).

Molecular Pharmacology Fast Forward. Published on July 28, 2020 as DOI: 10.1124/mol.120.119453
This article has not been copyedited and formatted. The final version may differ from this version.

Table 1. Saturation and competition studies using [^{3}H]DAMGO

Saturation	mMOR-1/mMOR-1G		
	+ Doxy (100 ng/ml) No mMOR-1G	−Doxy (0 ng/ml) With mMOR-1G	95% Confidence Interval
K_D (nM)	0.53 ± 0.01	0.41 ± 0.06	-0.00 to 0.25
B_{max} (fmol/mg protein)	33 ± 1.5	104 ± 6.8**	-84 to -58
Increase of B_{max}	315%		
Competition K_i (nM)			
Morphine	1.0 ± 0.1	0.9 ± 0.8	-1.8 to 1.6
DAMGO	0.5 ± 0.0	0.3 ± 0.0**	-0.26 to -0.14
M6G	6.1 ± 0.1	2.3 ± 0.4**	-5.1 to -2.5
B-Endorphin	22 ± 2.8	4.6 ± 0.4*	-26 to -10
Dynorphin A	706 ± 159	29 ± 24*	-1121 to -233.1

Saturation and competition assays were performed using indicated membranes as described in Materials and Methods. In saturation assays, five concentrations of [^{3}H]DAMGO (0.125 – 2 nM) were used. K_D values were calculated by nonlinear regression analyses (Prism 7). In competition assays, 1 – 1.5 nM of [^{3}H]DAMGO were used against three to four concentrations of unlabeled morphine and DAMGO (1 – 25 nM), M6G (5 – 100 nM), β-endorphin (10 – 200 nM) and dynorphin A (10 – 1000 nM). IC_{50} values were calculated by nonlinear regression analyses (Prism 7). K_i values were calculated by $K_i = IC_{50}/(1 + A/K_D)$, where A is the nM concentration of [^{3}H]DAMGO and

Molecular Pharmacology Fast Forward. Published on July 28, 2020 as DOI: 10.1124/mol.120.119453
This article has not been copyedited and formatted. The final version may differ from this version.

K_D value is obtained from saturation study. Results are the means ± SD of three independent experiments. Significant differences between – Doxy and + Doxy groups were analyzed by two-tailed Student's *t*-test. *: $p < 0.05$; **: $p < 0.01$.

Molecular Pharmacology Fast Forward. Published on July 28, 2020 as DOI: 10.1124/mol.120.119453
This article has not been copyedited and formatted. The final version may differ from this version.

Table 2. [^{35}S]GTPγS binding in Tet-Off cells expressing mMOR-1/mMOR-1G

	mMOR-1/mMOR-1G				
	+ Doxy (100 ng/ml) No mMOR-1G		− Doxy (0 ng/ml) With mMOR-1G		
	EC_{50} (μM)	% stim	EC_{50} (μM)	% stim	95% CI of % stim^
Morphine	0.2 ± 0.1	34 ± 5	0.3 ± 0.0	109 ± 24*	-145 to -5.5
Increase of % stim: ↑ 321%					
DAMGO	0.6 ± 0.1	63 ± 1	0.2 ± 0.0**	139 ± 19**	-124 to -27
Increase of % stim: ↑ 221%					
M6G	0.7 ± 0.5	43 ± 18	0.2 ± 0.0	91 ± 22*	-87 to -9.0
Increase of % stim: ↑ 212%					
B-Endorphin	0.8 ± 0.5	75 ± 16	0.9 ± 0.2	139 ± 71	-224 to 97
Increase of % stim: ↑ 183%					

[^{35}S]GTPγS binding was performed using membranes from – Doxy and + Doxy cells with six concentrations of indicated drugs (0 – 10 μM), as described in Materials and Methods. EC_{50} and % stimulation values over basal level (% stim) were calculated by nonlinear regression analysis (Prism 7). So, the basal level is, as always, 0%. Results are the means ± SD of three independent experiments. Significant differences between – Doxy and + Doxy groups were analyzed by two-tailed Student's *t*-test. *: $p < 0.05$; **: $p < 0.01$. ^: CI, Confidence Interval.

Molecular Pharmacology Fast Forward. Published on July 28, 2020 as DOI: 10.1124/mol.120.119453
This article has not been copyedited and formatted. The final version may differ from this version.

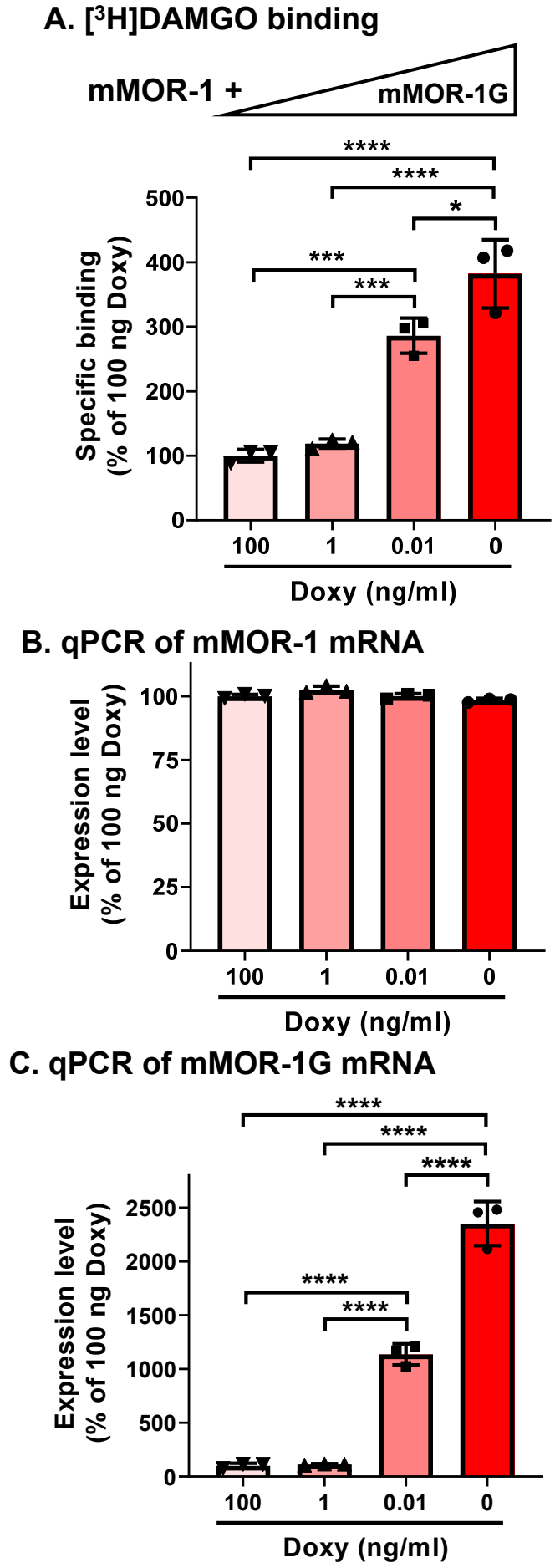

Fig. 1.

Molecular Pharmacology Fast Forward. Published on July 28, 2020 as DOI: 10.1124/mol.120.119453
This article has not been copyedited and formatted. The final version may differ from this version.

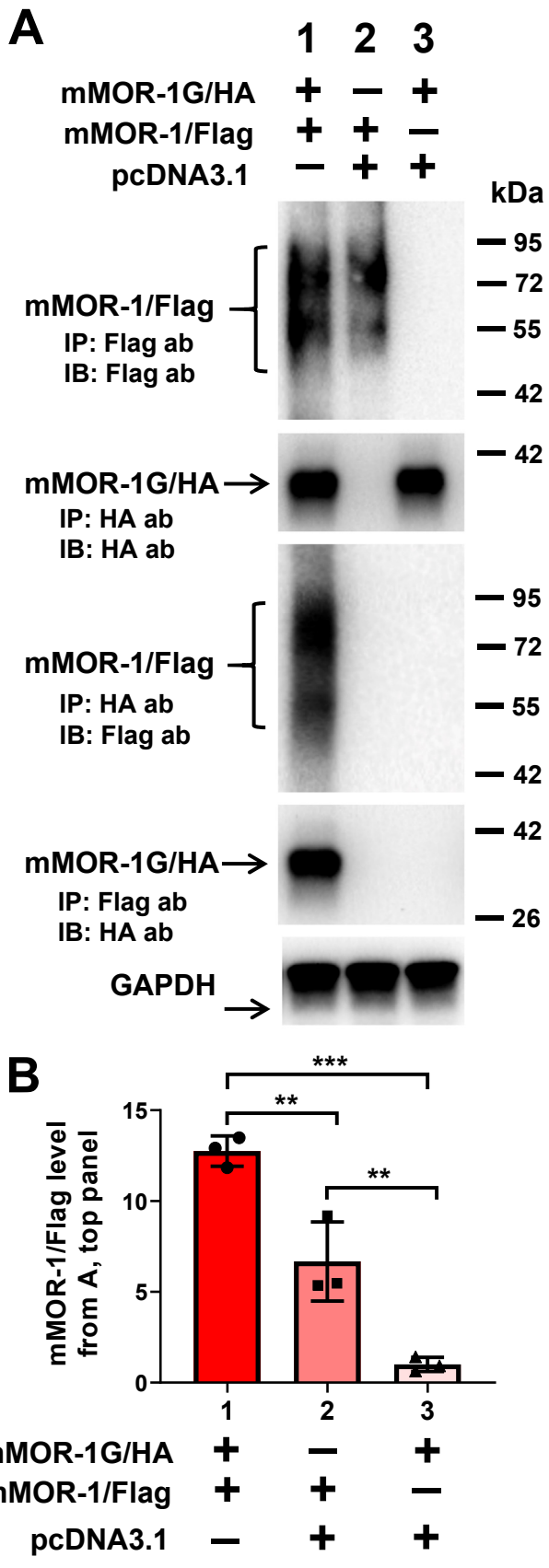

Fig. 2.

Molecular Pharmacology Fast Forward. Published on July 28, 2020 as DOI: 10.1124/mol.120.119453
This article has not been copyedited and formatted. The final version may differ from this version.

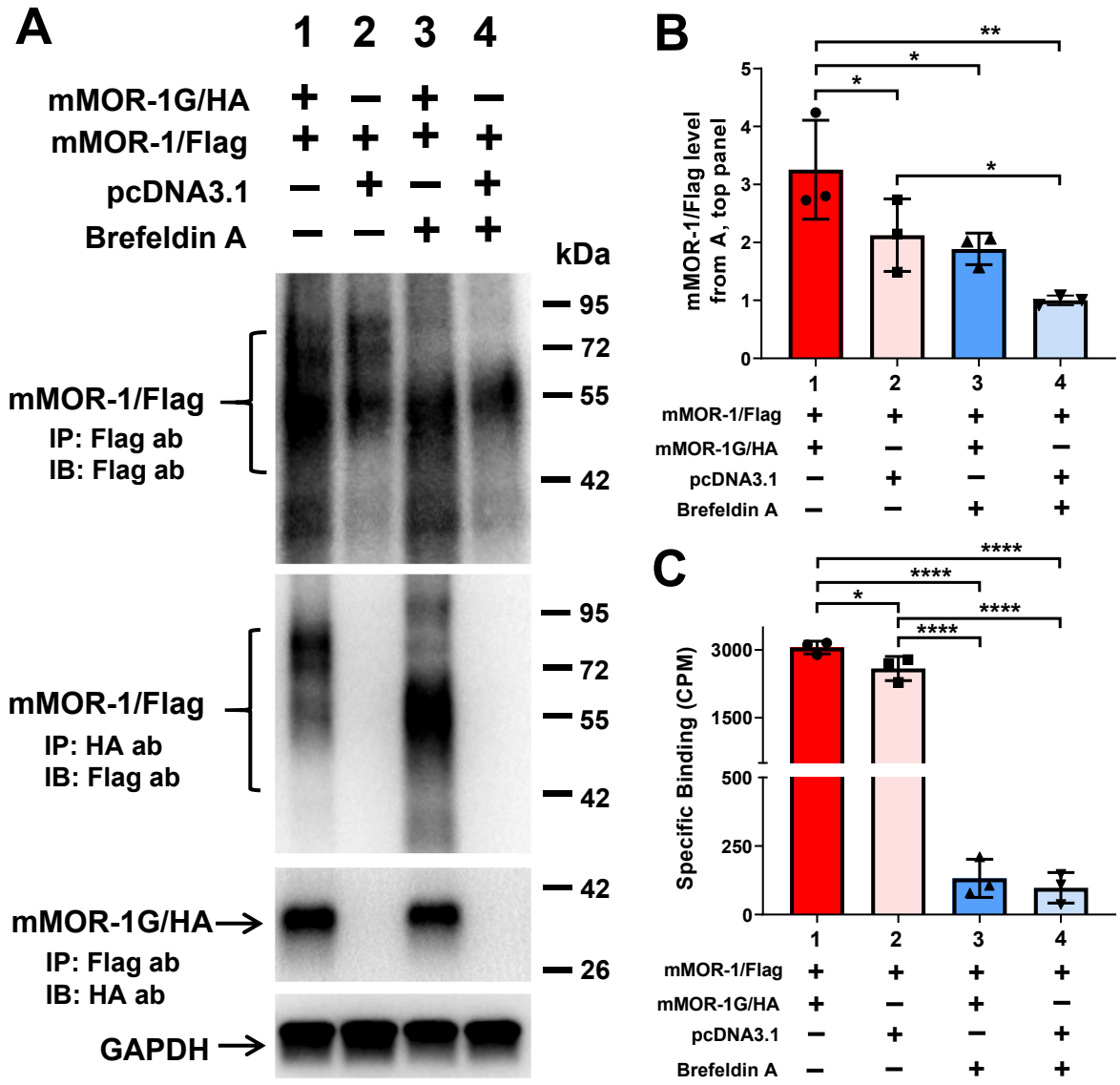

Fig. 3.

Molecular Pharmacology Fast Forward. Published on July 28, 2020 as DOI: 10.1124/mol.120.119453
This article has not been copyedited and formatted. The final version may differ from this version.

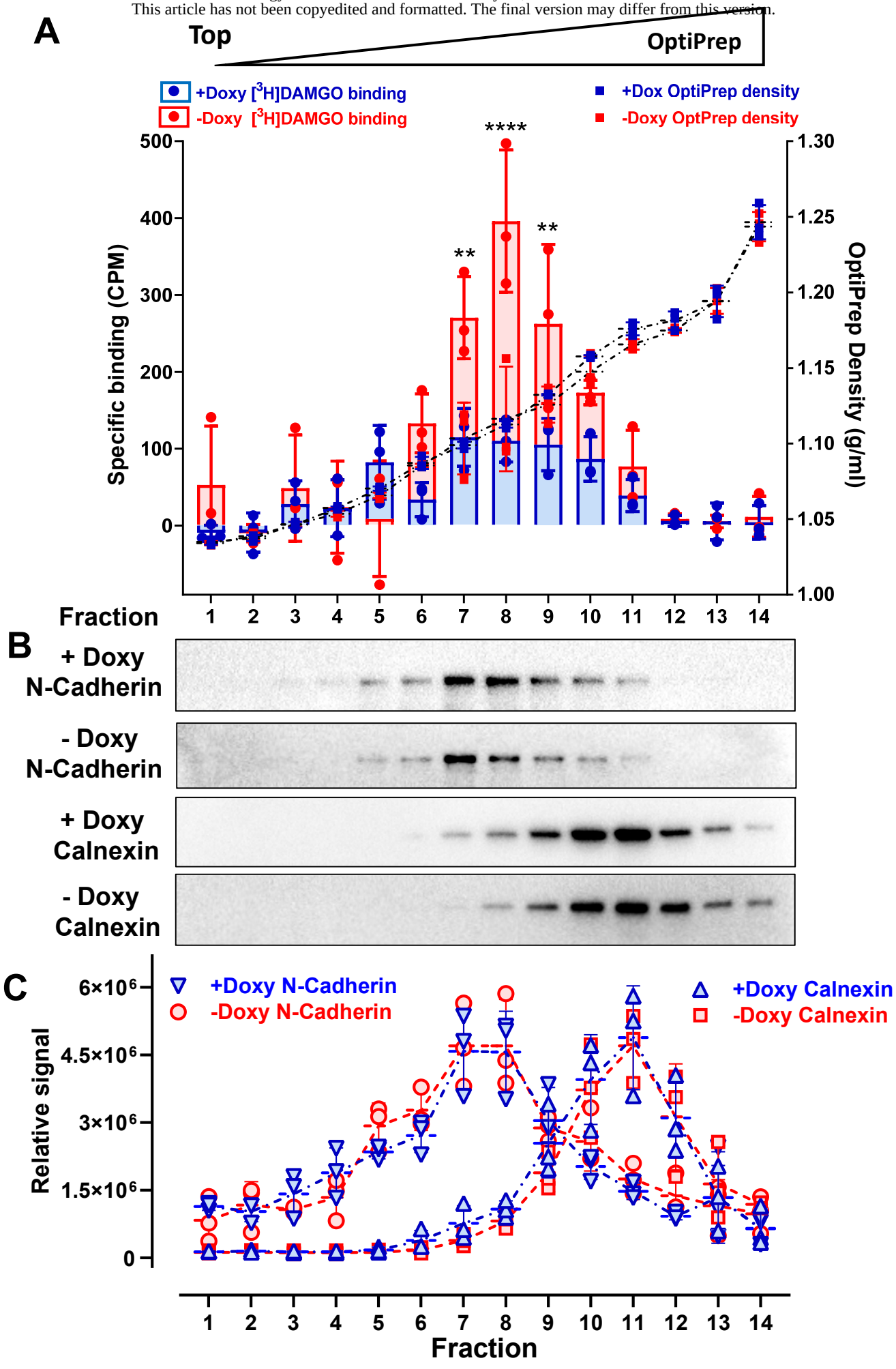

Fig. 4.